Synthesis of High-Surface-Area TiN/Carbon Composite Materials with Hierarchical Porosity via "Reactive Templating"

Anna Fischer, Young-Si Jun, Arne Thomas,* and Markus Antonietti

Colloid Department, Max Planck Institute of Colloids and Interfaces, Am Mühlenberg 1, D-14424 Potsdam-Golm, Germany

Received August 4, 2008. Revised Manuscript Received October 13, 2008

In this work, the synthesis of porous TiN/carbon composites via "reactive hard templating" is presented. The concept of this synthesis strategy is to use the template, responsible for the final morphology of the TiN/carbon material, as a reactant and nitrogen source; template removal is unnecessary as the final product is obtained as such. As reactive templates, two types of macroporous graphitic carbon nitride powders with different pore sizes (60 nm or 500 nm spherical pores) were used. The powders were infiltrated with a titanium precursor solution, aged for 1 night at 100 °C under air, and subsequently annealed at 800 °C to create the final nanocrystalline porous TiN/carbon structures. The final products were analyzed by XRD, TEM, HRTEM, EA, and gas sorption experiments. It was shown that the morphology of the resulting material generates from a nanocoating of the macropores of the carbon nitride reactive template, yielding aggregated hollow TiN/C spheres with hierarchical porosity.

Introduction

The design of complex porous materials was until recently limited to polymers,[1] carbons,[2,3] and oxidic material.[4−6] This is because oxides can be prepared by sol−gel chemistry,[7,8] which allows for templating techniques, such as with surfactants,[9] block copolymers,[10−14] or polymer latexes.[15] Postcrystallization of those amorphous layers gives the corresponding crystalline oxides[13,16−18] which are valuable functional materials. For the templating approaches, we differentiate the so-called soft templating, using organic templates such as surfactants or polymers as structure directing agents, from the so-called hard templating, where rigid silica, mineral, or carbon nanostructures are employed as porogenes.[19,20] It is obvious that the disadvantage of hard templating is the sometimes tedious removal of the template after material synthesis by etching techniques. On the other hand, all processes where material synthesis involves structural rearrangements at higher temperatures are automatically bound to hard templates. Recently, we introduced the concept of "reactive hard templating", which combines the advantages of hard templating with an in situ decomposition, i.e., removal of the template.[21,22] Here, the template is made of nanostructures of a solid state reactant which vanishes completely at elevated reaction conditions. This concept is especially useful for high-temperature transformations or the generation of structures that are sensitive against the etching conditions.

The synthesis of crystalline metal nitrides is such a high temperature procedure. Metal nitrides are traditionally produced by heating the corresponding metal with elemental nitrogen. This preparation method is highly energy consuming because long reaction times at elevated temperatures are required (T > 1300 °C) and leads usually to low surface area materials.[23] Nowadays, new synthetic strategies to high-surface-area metal nitrides are widely based on the conversion of metal oxide nanopowders into the corresponding nitride using nitrogen sources, such as ammonia[24−26] or hydrazine.[27,28]

However, most of the reports concerning metal nitrides nanostructures are dealing with nanoparticles and only a few

* Corresponding author. E-mail: arne.thomas@mpikg.mpg.de.

(1) Thomas, A.; Goettmann, F.; Antonietti, M. *Chem. Mater.* **2008**, *20*, 738.
(2) Ryoo, R.; Joo, S. H.; Kruk, M.; Jaroniec, M. *Adv. Mater.* **2001**, *13*, 677.
(3) Lee, J.; Kim, J.; Hyeon, T. *Adv. Mater.* **2006**, *18*, 2073.
(4) Ciesla, U.; Schuth, F. *Microporous Mesoporous Mater.* **1999**, *27*, 131.
(5) Schuth, F.; Schmidt, W. *Adv. Mater.* **2002**, *14*, 629.
(6) Polarz, S.; Antonietti, M. *Chem. Commun.* **2002**, 2593.
(7) Livage, J.; Henry, M.; Sanchez, C. *Prog. Solid State Chem.* **1988**, *18*, 259.
(8) Livage, J.; Beteille, F.; Roux, C.; Chatry, M.; Davidson, P. *Acta Mater.* **1998**, *46*, 743.
(9) Kresge, C. T.; Leonowicz, M. E.; Roth, W. J.; Vartuli, J. C.; Beck, J. S. *Nature* **1992**, *359*, 710.
(10) Attard, G. S.; Glyde, J. C.; Goltner, C. G. *Nature* **1995**, *378*, 366.
(11) Bagshaw, S. A.; Prouzet, E.; Pinnavaia, T. J. *Science* **1995**, *269*, 1242.
(12) Zhao, D. Y.; Huo, Q. S.; Feng, J. L.; Chmelka, B. F.; Stucky, G. D. *J. Am. Chem. Soc.* **1998**, *120*, 6024.
(13) Smarsly, B.; Antonietti, M. *Eur. J. Inorg. Chem.* **2006**, 1111.
(14) Thomas, A.; Schlaad, H.; Smarsly, B.; Antonietti, M. *Langmuir* **2003**, *19*, 4455.
(15) Antonietti, M.; Berton, B.; Goltner, C.; Hentze, H. P. *Adv. Mater.* **1998**, *10*, 154.
(16) Grosso, D.; Boissiere, C.; Smarsly, B.; Brezesinski, T.; Pinna, N.; Albouy, P. A.; Amenitsch, H.; Antonietti, M.; Sanchez, C. *Nat. Mater.* **2004**, *3*, 787.
(17) Brezesinski, T.; Groenewolt, M.; Pinna, N.; Amenitsch, H.; Antonietti, M.; Smarsly, B. M. *Adv. Mater.* **2006**, *18*, 1827.
(18) Schuth, F. *Chem. Mater.* **2001**, *13*, 3184.
(19) Tiemann, M. *Chem. Mater.* **2008**, *20*, 961.
(20) Lu, A. H.; Schuth, F. *Adv. Mater.* **2006**, *18*, 1793.
(21) Fischer, A.; Antonietti, M.; Thomas, A. *Adv. Mater.* **2007**, *19*, 264.
(22) Fischer, A.; Müller, J. O.; Antonietti, M.; Thomas, A. *ACS Nano.* **2008**, DOI: 10.1021/nn800503a.
(23) Toth, L. E. *Transition Metal Carbides and Nitrides*; Academic Press: New York, 1971.

10.1021/cm802127t CCC: $40.75
Published on Web 11/21/2008

reports are known concerning porous metal nitrides.[25,26,29−32] In this work, we report on "reactive hard templating" toward complex macroporous TiN structures. Such a porous, high-surface-area titanium nitride has considerable prospects as catalyst,[31,33,34] or as catalyst support.[35] The "reactive hard template" has to play two roles in the synthesis. First it has to act as a template, imprinting its morphology to the resulting nitride, and second, it has to act through its thermal decomposition as a nitrogen source for the formation of the final TiN. This implies that metal nitride formation temperature has to be in the same range as the reactive template decomposition. One adequate candidate as reactive template material for the synthesis of metal nitrides is graphitic C_3N_4, as demonstrated by the synthesis of metal nitride nanoparticles in and through the thermal decomposition of mesoporous g-C_3N_4.[21,36,37] This work is an extension of this concept to metal nitride porous structures using macroporous g-C_3N_4 materials as reactive templates for the synthesis of macroporous TiN materials.

Two types of macroporous g-C_3N_4 materials were used as reactive hard templates: one with 60 nm spherical pores, the other with 500 nm spherical pores, resulting in the formation of porous TiN structures with 55 and 450 nm pores, respectively, and high surface areas.

Experimental Section

All chemicals were used as received without any purification.

Silica Templates for the Synthesis of Macroporous C_3N_4. Synthesis of 60 nm silica spheres (ST-60): The silica nanoparticle were synthesized by a slight modification of the approach described by Johnson et al.[38] A microemulsion was prepared by rapidly stirring 150 mL of cyclohexane, 6 mL of *n*-hexanol, 19 mL of Triton NP-9, 7 mL of water, and 1.7 mL of 28% aqueous ammonia. To this solution was added 10 mL of tetraethylorthosilicate (TEOS, Aldrich). The mixture was stirred at ambient temperature for 2 days. Most of the solvent was removed by rotary evaporation. The obtained viscous gel was then calcined at 200 °C for 2 h, at 350 °C for 3 h, and at 550 °C for 5 h. A white powder composed of highly monodispersed silica particles with a diameter of 60−65 nm was obtained. Five-hundred nanometer spheres (Monospheres 500 (ST-500)) were kindly provided by Merck.

Synthesis of Macroporous Graphitic C_3N_4. Synthesis of macroporous graphitic C_3N_4 with 60 nm pores (CN-60): The 60 nm silica particles (ST60) were pressed into a pellet and annealed at 800 °C for 5 h. The cooled pellet was infiltrated with molten cyanamide (Aldrich). To achieve a perfect infiltration of the pellet with the carbon nitride precursor, the pellet was placed in a vacuum oven for 10 min at 40 °C. The infiltrated pellet was then placed in a covered crucible and heated to 550 °C for 5 h with a heating ramp of 2.2 °C min^{-1}. To remove the silica template, the resulting yellow pellet was shaken in an aqueous 4 M NH_4HF_2 solution for 2 days. The powder was collected by centrifugation, redispersed and shaken in distilled water for two days to be finally washed with ethanol. After the drying in a vacuum oven at 70 °C (overnight), a macroporous yellow powder was obtained.

Synthesis of macroporous graphitic carbon nitride with 500 nm pores (CN-500): 1 g of M500 was dispersed in 5 g of molten cyanamide (Aldrich) and 2 g of water by high power sonication and calcined at 550 °C for 4 h, with a heating ramp of 2.2 °C min^{-1}. The resulting yellow powder was then treated with NH_4HF_2, water, and ethanol as described for the sample CN-60. ***Caution!*** *NH_4HF_2 causes severe burns in contact with skin. Appropriate gloves, clothing, and shoes should be worn during handling and chemicals should be handled only in a chemical fume hood.*

Synthesis of Macroporous TiN/Carbon Nanocomposites. The porous carbon nitride powder (CN-60 or CN-500) was infiltrated with a titanium tetrachloride/ethanol solution with the mass ratio: $TiCl_4$/EtOH = 2.3 g/5 g. The infiltrated powder was filtered off and aged at 100 °C under air for 1 night. Finally the aged powder was heated in a closed crucible under nitrogen flow to 800 °C for 3 h. When the oven was cooled to room temperature, the samples were removed from the oven. ***Caution!*** *The thermal decomposition of C_3N_4 yields the production of toxic gases such as HCN. Thus, ovens have to be placed in a fume hood or places with sufficient ventilation.*

Results and Discussion

TiN/C Macroporous Foam. Because graphitic carbon nitrides (g-C_3N_4) can act as nitrogen source,[39,40] releasing nitrogen in the form of ammonia and hydrogen cyanide during their thermal decomposition, they can also be used as templates for the synthesis of nanostructured metal nitrides. This was illustrated in previous work for the synthesis of metal nitride nanoparticles from mesoporous graphitic carbon nitride.[21,22] Here, we will focus on the synthesis of a macroporous TiN/Carbon foam by using a macroporous graphitic carbon nitride as the reactive template. Although the synthesis of the metal nitride nanoparticles was based on nanocasting, it will be shown that in this case, the resulting TiN/Carbon foam results from a nanocoating[41] on the carbon nitride support, i.e., the pores are not completely filled with the titania precursor. The used graphitic carbon nitride template is a macroporous graphitic carbon nitride (CN-60) with spherical pores of 60−65 nm in diameter and a wall thickness between 10 and 30 nm, obtained through hard templating of similar sized silica spheres. As can be seen from the comparison of the TEM images (Figure 1) of the silica particles and the resulting macroporous g-C_3N_4,

(24) Claridge, J. B.; York, A. P. E.; Brungs, A. J.; Green, M. L. H. *Chem. Mater.* **2000**, *12*, 132.
(25) Krawiec, P.; De Cola, P. L.; Glaser, R.; Weitkamp, J.; Weidenthaler, C.; Kaskel, S. *Adv. Mater.* **2006**, *18*, 505.
(26) Panda, R. N.; Kaskel, S. *J. Mater. Sci.* **2006**, *41*, 2465.
(27) Jacob, K. T.; Verman, R.; Mallya, R. M. *J. Mater. Sci.* **2002**, *37*, 4465.
(28) Vogt, K. W.; Naugher, L. A.; Kohl, P. A. *Thin Solid Films* **1995**, *256*, 106.
(29) Krawiec, P.; Panda, R. N.; Kockrick, E.; Geiger, D.; Kaskel, S. *J. Solid State Chem.* **2008**, *181*, 935.
(30) Hong, Y. C.; Uhm, H. S. *Scr. Mater.* **2008**, *59*, 262.
(31) Fischer, A.; Makowski, P.; Müller, J. O.; Antonietti, M.; Thomas, A.; Goettmann, F. *ChemSusChem* **2008**, *1*, 444.
(32) Chaplais, G.; Kaskel, S. *J. Mater. Chem.* **2004**, *14*, 1017.
(33) Kaskel, S.; Schlichte, K.; Kratzke, T. *J. Mol. Catal. A: Chem.* **2004**, *208*, 291.
(34) Kaskel, S.; Schlichte, K.; Chaplais, G.; Khanna, M. *J. Mater. Chem.* **2003**, *13*, 1496.
(35) Musthafa, O. T. M.; Sampath, S. *Chem. Commun.* **2008**, 67.
(36) Goettmann, F.; Fischer, A.; Antonietti, M.; Thomas, A. *Angew. Chem., Int. Ed.* **2006**, *45*, 4467.
(37) Thomas, A.; Fischer, A.; Goettmann, F.; Antonietti, M.; Müller, J. O.; Schlögl, R.; Carlsson, J. *J. Mater. Chem* **2008**, *18*, 4893.
(38) Johnson, S. A.; Ollivier, P. J.; Mallouk, T. E. *Science* **1999**, *283*, 963.
(39) Kawaguchi, M.; Nozaki, K. *Chem. Mater.* **1995**, *7*, 257.
(40) Zhao, H. Z.; Lei, M.; Yang, X.; Jian, J. K.; Chen, X. L. *J. Am. Chem. Soc.* **2005**, *127*, 15722.
(41) Caruso, R. A.; Antonietti, M. *Chem. Mater.* **2001**, *13*, 3272.

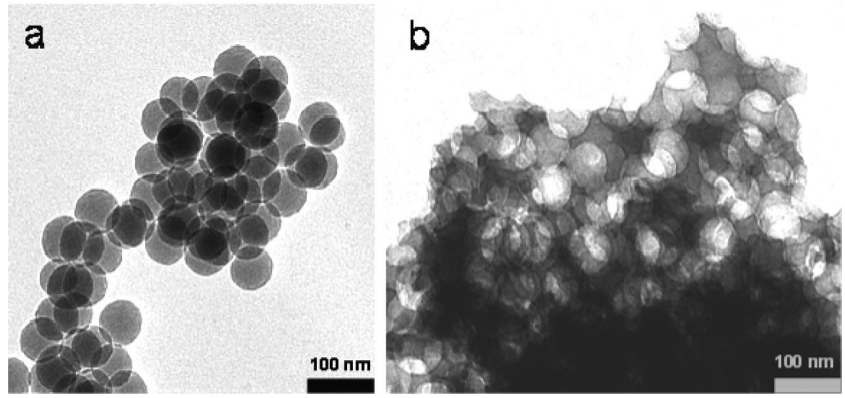

Figure 1. TEM micrographs of (a) 60 nm silica particles (ST-60) used as template for the synthesis of (b) a macroporous g-C_3N_4 with 60 nm spherical pores (CN-60).

the pore network of the CN-60 sample reflects perfectly the shape and size of the used silica template. After removal of the template, the sample CN-60 shows the typical features of a graphitic carbon nitride, as shown in the XRD pattern (see the Supporting Information, Figure S1), namely, a graphitic stacking peak at 27.3°, as well as a peak at 13.1° resulting from the periodic arrangement of the condensed tri-*s*-triazine units in the sheets. From nitrogen sorption the surface area of the sample was determined to be 65 m^2/g (BET, Figure 6), which goes well with the calculations for a macroporous material with 60 nm pores.

The macroporous metal nitride was produced using a dilute metal precursor solution, which in combination with the large pores in the carbon nitride template ensures a partial filling of the pores, only.

Because of the chemical affinity of titanium for amine functions, we can assume that the titania precursor layer is bound to the surface of the carbon nitride pores through the coupling with nitrogen. The infiltrated powder was aged for 1 night at 100 °C, first of all to evaporate the ethanol, but second to induce a partial condensation of the titania-orthoesters in the presence of the air moisture inside the pores. The subsequent heat treatment at 800 °C under nitrogen results in a decomposition of porous carbon nitride into NH_3 and CN_x gases (as verified by TGA-mass spectroscopy, see the Supporting Information, Figure S2). Reaction of those in situ fragments with the titania precursor results in a nanocrystalline, highly porous powder. Its XRD pattern (Figure 2, here TiN-60) could be indexed in agreement with the diffraction peaks observed for osbornite (TiN, space group $Fm\bar{3}m$, cell parameter: $a = b = c = 4.235$ Å, $\alpha = \beta = \gamma = 90°$).[42] The observed diffraction peaks are rather broad, indicating that the TiN-60 powder is composed of osbornite nanocrystals. Applying the Scherrer equation to the most intensive diffraction peak (200) gives an average crystallite size of around 7 nm. Beside the presence of osbornite, 30 wt % residual carbon could be detected in TiN-60 by elemental analysis. Thus the material TiN-60 is probably better described as TiN/Carbon nanocomposite, i.e., here, TiN nanoparticles glued together in a disordered carbon matrix.

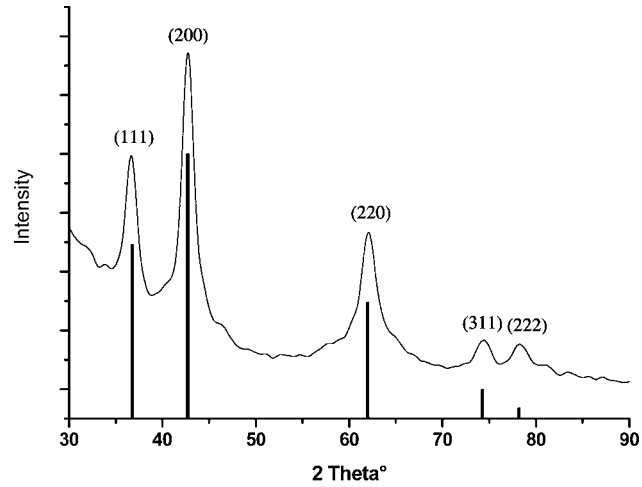

Figure 2. X-Ray diffraction pattern of the macroporous TiN/carbon composite TiN-60. The black lines represent the peak positions from the ICSD database for the osbornite phase.

The texture of the sample was investigated by SEM and TEM measurements. Figures 3 and 4 compare images of the starting macroporous graphitic carbon nitride (CN-60) and the resulting titanium nitride/carbon powder (TiN-60). Both materials are obviously highly porous, while the pores of the TiN-60 sample [Ø ≈ 47−55 nm] are about 10 nm smaller than the pores observed in the starting material CN-60 [Ø ≈ 60−65 nm]. This is accompanied with an overall shrinking of the dimensions of the material. The TEM pictures also indicate that the pore walls of the TiN-60 sample are much thinner than those of the CN-60 sample, as can be seen from the TEM images, which is most presumably due to the formation of a nanocoating layer on the pore walls, which is then transcribed into the TiN.

Selected area electron diffraction (SAED) (inset in Figure 4) confirms the XRD observation that the observed porous structure is composed of crystalline osbornite. The observed diffraction rings exactly corresponds to the expected lattice spacing of the osbornite crystal phase. The particulate character of the pore walls is also indicated in high-resolution SEM (Figure 3c), where the single TiN nanocrystallites become visible. HRTEM measurements (Figure 5) again confirm that the pore walls are composed of 5−7 nm crystallites with well-developed lattice fringes.

(42) Hasegawa, M.; Yagi, T. *J. Alloys Compd.* **2005**, *403*, 131.

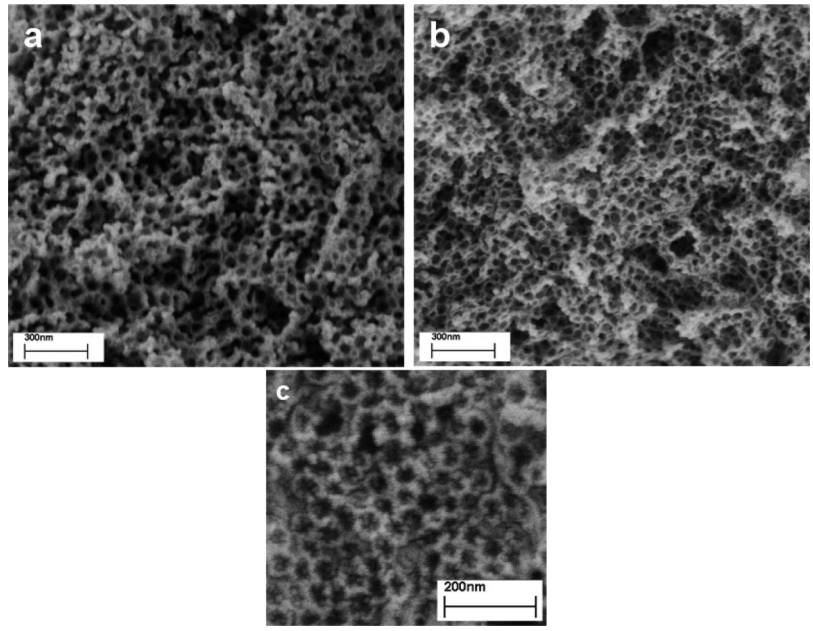

Figure 3. SEM images of (a) the starting macroporous carbon nitride CN-60 and (b, c) the resulting macroporous TiN/Carbon composite TiN-60.

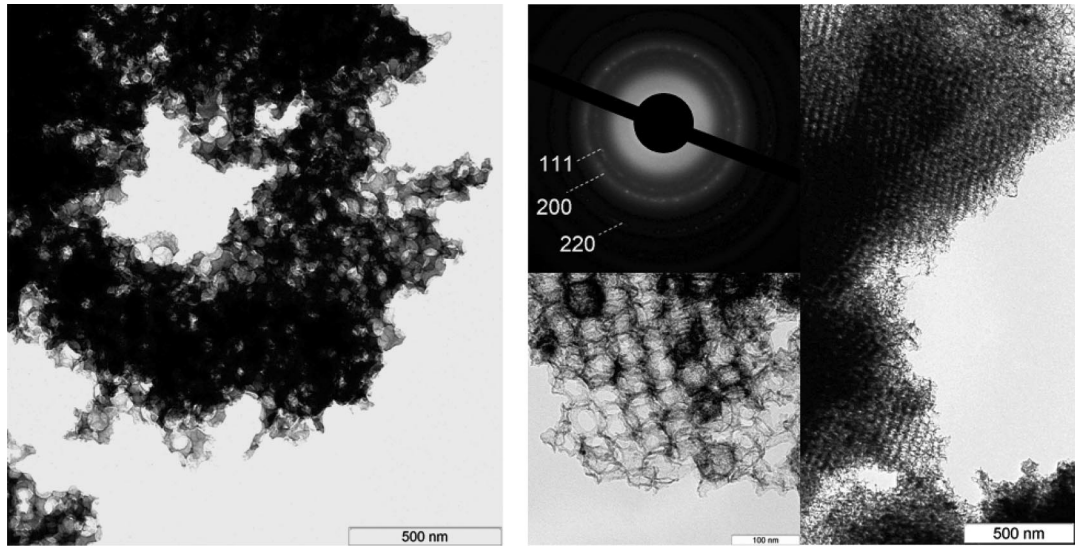

Figure 4. TEM images of the macroporous graphitic carbon nitride CN-60 (left) and the TiN/carbon composite TiN-60; upper inset: selected area electron diffraction (SAED).

Fast Fourier transformation of the selected area in Figure 5 results in a determined distance of 2.119 Å, as compared with the database reported lattice distance $d_{(200)} = 2.117$ Å of the TiN osbornite phase. HRTEM also supports our view that the TiN nanocrystals are embedded in an amorphous carbon matrix. EDX measurements on the pore walls confirm the presence of titanium in the walls (peak at 4550 eV and at 4950 eV).

The surface area and the apparent mesopore volume of the TiN-60 sample were investigated by nitrogen sorption measurements and compared to the values of the macroporous CN-60 samples (Figure 6). While the isotherm for the CN-60 points to a predominantly macroporous material, isotherms of the TiN-60 sample indicate to an additionally micro- and mesoporous material with a hysteresis in the relative pressure range $0.43 < p/p_o < 1$. The comparison of the two samples also gives a big difference in the measured surface area and apparent pore volume. The TiN-60 powder exhibits a rather high surface area of 330 m^2/g and an apparent mesopore volume of 0.76 cm^3/g, which is five times bigger than the obtained values for the starting CN-60 carbon nitride template (surface area of 65 m^2/g and apparent pore volume of 0.167 cm^3/g).

An explanation for the significant increase in surface area and porosity is shown in Scheme 1: thermal decomposition of the formerly dense carbon nitride walls releases nitrogen rich gases, which transform the titania coating into TiN. The final nanostructure can be understood as an interconnected TiN/Carbon composite made up of 50 nm sized hollow spheres. These spheres thus exhibit an internal porosity comparable to the pores found in the carbon nitride template. However, the much thinner pore walls plus an additional porosity created by interstitial sites between the hollow spheres yield an overall higher surface area and porosity.

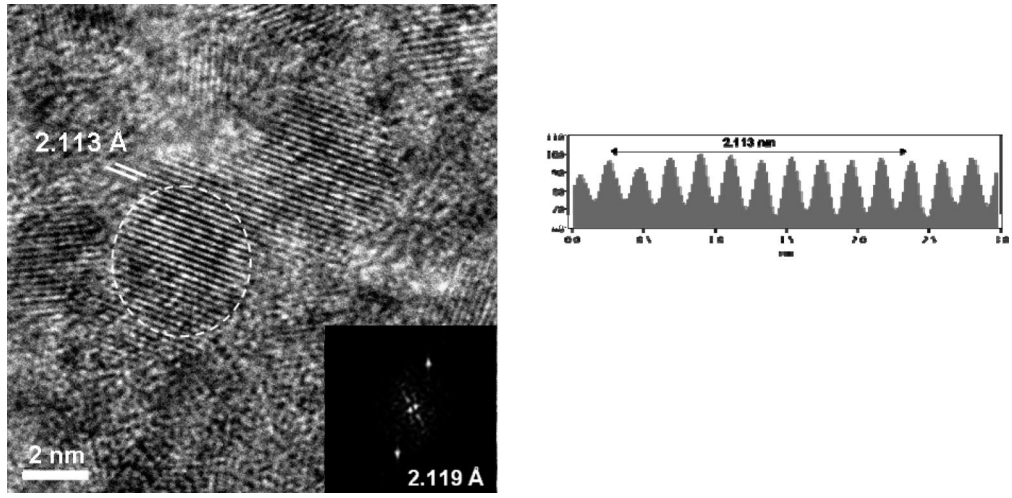

Figure 5. HRTEM pictures from the macroporous TiN/carbon composite TiN-60. The inset inlet represents the reduced FFT of the delimited area. A lattice distance of 2.11 Å, corresponding to the lattice distances d_{200} of the osbornite phase, could be determined.

Scheme 1. Schematic Model of the Formation of the Macroporous Titanium Nitride/Carbon Composite Starting from Macroporous Carbon Nitride

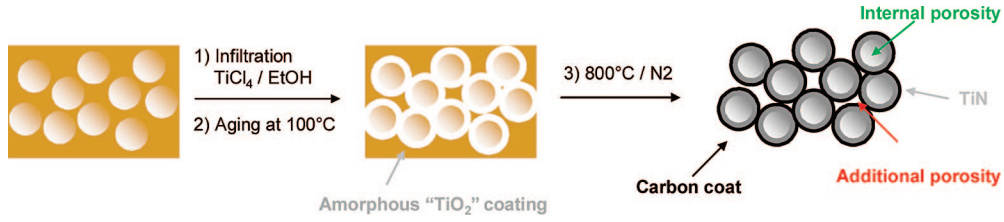

Furthermore, the nanoparticulate structure of the pore walls in the TiN-60 sample essentially constitutes the high surface area through the creation of supplementary interface. It should be furthermore noted that the amorphous carbon matrix will also certainly contribute to the overall surface area.

Synthesis of Foams with Larger Pores. Using the same synthetic strategy, a macroporous TiN with pores 500 nm in diameter was synthesized from CN-500, a macroporous carbon nitride with ~500 nm pores and a wall thickness between 10−50 nm. SEM micrographs of the C_3N_4 template CN-500 and the porous TiN-500 derived therefrom are shown in Figure 7. The obtained TiN powder TiN-500 is composed of spheres with 450−470 nm diameter, intergrown to a particle-based network. Higher-magnification illustrates that the spheres are hollow and apparently composed of TiN nanocrystallites.

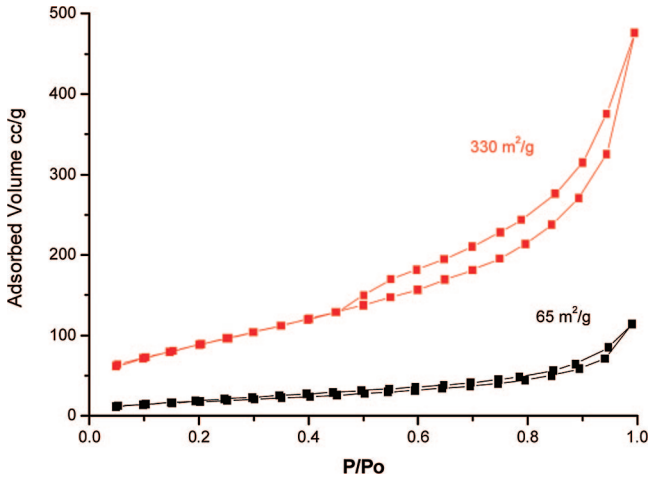

Figure 6. Nitrogen sorption isotherm adsorption and desorption branch of the starting carbon nitride template/nitriding agent CN-60 (black) and the resulting titanium nitride/carbon composite TiN-60 (red).

The obtained material is composed of cubic crystalline TiN, as confirmed by XRD (see the Supporting Information, Figure S3). The peaks are again broad and indicative for the presence of TiN nanocrystallites; the Scherrer equation applied to the most intense (200) peak gives an average crystallite size of 7 nm in size. Interestingly, elemental analysis indicates that there is practically no residual carbon left in this structure. It seems that in the case of the CN-500 sample, the thin wall (10−50 nm) in combination with the large pore size (480−500 nm), compared to the CN-60 sample with pores of only 60−65 nm in size, ensures a quantitative reaction between the metal precursor and the nitrogen donor matrix, yielding significant reduction of the carbon content. Indeed, through the higher ratio pore volume/wall thickness, a higher overall ratio Ti/C_3N_4 can be assumed upon infiltration of the titania precursor. Previous work has shown that the amount of residual carbon depends on the ratio of preceding TiO_2/C_3N_4,[31] which explains the finding that no residual carbon is left in the TiN-500 material.

The hollow character of the spheres and the inner nanoparticulate structure was additionally confirmed by TEM (Figure 8). HRTEM evidence by the presence of well-developed lattice fringes that the nanoparticles, the building blocks of the walls, are highly crystalline (Figure 8 c). As in the case of the TiN-60 sample, the morphology of the resulting TiN powder is a result of the morphology of the

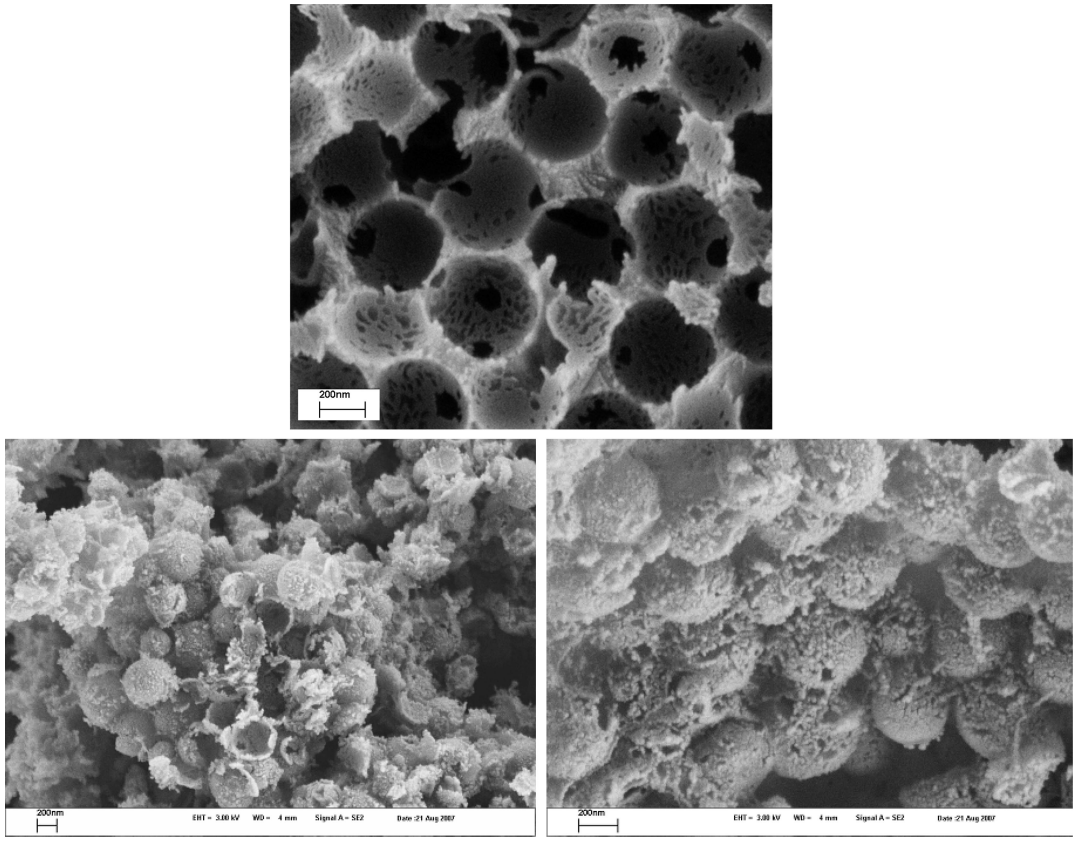

Figure 7. SEM images of the macroporous carbon nitride template with 500 nm pores (CN-500) (top) and the obtained TiN-500 (bottom). The magnified image (bottom right) shows the nanoparticulate structure of the sphere walls.

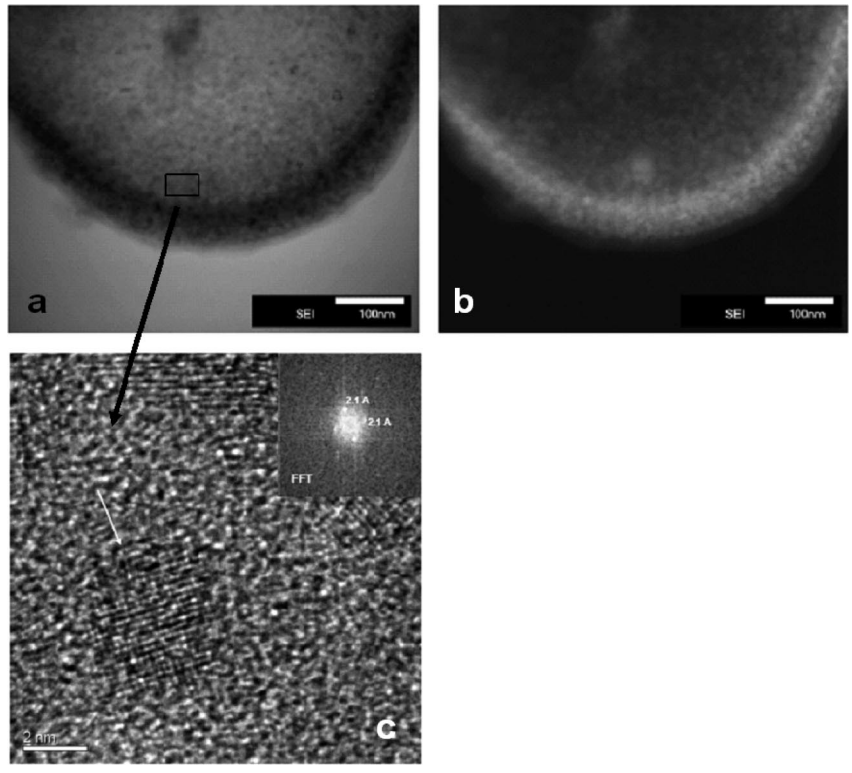

Figure 8. (a) Bright-field and (b) dark-field STEM measured on one isolated TiN hollow sphere. (c) HRTEM image shows that the sphere wall is composed of small (5−7 nm in size) TiN nanocrystals.

starting carbon nitride template. A comparison of the starting macroporous network of the carbon nitride with the final hollow spheres, in terms of shape and size, clearly indicates that the morphology of the TiN hollow spheres is a transcription of the shape and size of the carbon nitride pores. The porosity of the obtained TiN-500 hollow sphere powder

was investigated via nitrogen sorption measurements. The TiN powder has a surface area of 143 m^2/g and an apparent pore volume of 0.66 cm^3/g, whereas the starting carbon nitride CN-500 has only 16 m^2/g surface areas and an apparent pore volume of 0.06 cm^3/g (see the Supporting Information, Figure S4). This behavior repeats the behavior of the TiN-60 sample and is explained according to the same model.

Conclusion

It was shown that employment of graphitic carbon nitride nanostructures as reactive hard templates enables the direct synthesis of high-surface-area titanium nitride/carbon nanostructures. The resulting nanostructure is similar in architecture to the starting carbon nitride, but because of the much thinner pore walls and an additional porosity created by the interstitial sites of the hollow TiN/C spheres, the specific surface area of the resulting TiN/carbon composites increased by a factor 5, also bringing micro- and mesopores into the structure. This is potentially beneficial for applications, such as catalysis, as such materials with hierarchical porosity provide the large surface area of mesoporous materials and combine it with the excellent transport through macroporous materials.

The comparison of the different materials shows that the amount of side product of the decomposition of carbon nitride, amorphous carbon, can be adjusted by the relative amount of template and metal phase and its dispersion. For big pores and thin metal oxide layers, a pure TiN practically without any carbon residue is formed. For practical applications, however, it stays an open question how much carbon binder is optimal, as, for instance, thin carbon coating of nanoscopic battery materials turned out to improve lifetime and conductivity.[43]

As nitrification of metal oxides by carbon nitride decomposition is not restricted to titania, but seems to be rather practical for many metal oxides, we think that the present process can be generalized for the synthesis of many porous binary and ternary metal nitrides of choice.

Acknowledgment. The Max Planck Society is acknowledged for financial support within the EnerChem network.

Supporting Information Available: X-Ray diffraction pattern of the macroporous graphitic carbon nitride CN-60 and TGA-mass spectroscopy measurement of bulk graphitic C_3N_4 (PDF). This material is available free of charge via the Internet at http://pubs.acs.org.

CM802127T

(43) Hu, Y. S.; Demir-Cakan, R.; Titirici, M. M.; Muller, J. O.; Schlogl, R.; Antonietti, M.; Maier, J. *Angew. Chem., Int. Ed.* **2008**, *47*, 1645.